POLITECNICO DI TORINO
Repository ISTITUZIONALE

Atmospheric-pressure plasma jet texturing of C/C composites for improved joint strength

Original
Atmospheric-pressure plasma jet texturing of C/C composites for improved joint strength / De Zanet, Alessandro; Valenza, Fabrizio; Casalegno, Valentina; Gambaro, Sofia; D'Isanto, Fabiana; Salvo, Milena. - In: CERAMICS INTERNATIONAL. - ISSN 0272-8842. - 50:20, Part B(2024), pp. 38933-38942. [10.1016/j.ceramint.2024.07.257]

Availability:
This version is available at: 11583/2991263 since: 2024-07-29T08:39:27Z

Publisher:
Elsevier

Published
DOI:10.1016/j.ceramint.2024.07.257

Terms of use:

This article is made available under terms and conditions as specified in the corresponding bibliographic description in the repository

Publisher copyright

(Article begins on next page)

08 December 2024

Ceramics International 50 (2024) 38933–38942

Contents lists available at ScienceDirect

Ceramics International

journal homepage: www.elsevier.com/locate/ceramint

Atmospheric-pressure plasma jet texturing of C/C composites for improved joint strength

Alessandro De Zanet [a,*], Fabrizio Valenza [b], Valentina Casalegno [a], Sofia Gambaro [b], Fabiana D'Isanto [a], Milena Salvo [a]

[a] Department of Applied Science and Technology (DISAT) Politecnico di Torino, Torino, Italy
[b] National Research Council – Institute of Condensed Matter Chemistry and Technologies for Energy (CNR-ICMATE), Genova, Italy

ARTICLE INFO

Handling Editor: Dr P. Vincenzini

ABSTRACT

This study explores the use of air-fed atmospheric pressure plasma jets (APPJs) as a pre-joining treatment for 3D carbon fiber-reinforced carbon matrix composites (C/C) with the aim of both creating a textured surface that resembles a brush structure and improving the joint strength.

The effects of various treatment time lengths on the mass loss, etching depth, and surface texture were investigated using SEM and confocal microscopy. An optimal process time of 30 s was selected, while keeping the other process parameters fixed (air flow of 1750 l/h and nozzle-sample distance of 5 mm). Wetting tests were conducted at 1000 °C, on both untreated and pre-treated C/C surfaces by means of liquid TiCuNi brazing alloy, and low contact angles of about 20° were measured. C/C–TiCuNi–C/C and C/C–TiCuNi–Cu joints were then produced, and their interfacial reactivity was evaluated. The apparent shear strength measured for the APPJ-treated C/C–Cu joints was 140 % higher than the value recorded for the untreated joints, thus confirming the effectiveness of the treatment.

Even though a further investigation is needed in which an optimization of the process parameters should be included, this preliminary study has revealed the viability of APPJ as a promising technique to enhance the bonding of C/C composites in dissimilar assemblies and to improve the joint quality.

1. Introduction

Carbon-fiber reinforced carbon matrix composites (C/C) stand out among Ceramic Matrix Composites (CMCs) because of their applicability in high-temperature environments, which can be as high as 2800 °C if they are protected from oxidation. These materials exhibit remarkable resistance to thermal shock, maintain their mechanical strength at extremely high temperatures, and have high thermal conductivity and low density [1]. Initially considered for the plasma-facing material in nuclear fusion ITER divertor armor, they were eventually replaced by tungsten due to certain limitations (e.g. high tritium retention, fibers are heavily eroded under intense heat fluxes and thermal-induced stresses can damage the fiber integrity) [2,3]. These materials were then coupled with a copper alloy heat sink to ensure effective heat removal, particularly for such applications as nuclear fusion in ITER. The challenge of achieving effective bonding and a high thermal transfer from C/C to copper has prompted research into finding feasible joining techniques. Brazing has emerged as the preferred option to withstand the high heat flux within a joint, as mechanical solutions were deemed ineffective for efficient heat dissipation [4–6]. The exploration of dissimilar joints has not been confined to this specific application, and has also found relevance in the aerospace sector. In fact, C/C can be used to address the severe thermal conditions experienced during space missions, including such tasks as the thermal management of nozzles and re-entry operations. Consequently, despite the temporary cessation of their development as plasma-facing armor material in the ITER project, efforts have persisted in the joining technology domain. Indeed, the investigation of new brazing processes and the refinement of established methods have been witnessed in recent years [7–9]. This sustained research is aimed at enhancing the capabilities of C/C composites used in aerospace applications, and at ensuring their resilience and effectiveness in managing the extreme thermo-physical challenges encountered in the demanding environments of space missions.

Surface topography is a critical factor that influences both the

* Corresponding author.
E-mail address: alessandro.dezanet@polito.it (A. De Zanet).

https://doi.org/10.1016/j.ceramint.2024.07.257
Received 26 April 2024; Received in revised form 17 July 2024; Accepted 18 July 2024
Available online 20 July 2024
0272-8842/© 2024 The Authors. Published by Elsevier Ltd. This is an open access article under the CC BY-NC-ND license (http://creativecommons.org/licenses/by-nc-nd/4.0/).

wettability and the coupling between a substrate and the joining material. If the surface texture facilitates anchoring between the adherend and the adhesive, a mechanical interlocking effect may occur. This effect arises when the joining materials infiltrate valleys that are present on the surface. These regions act as anchoring bridges, as they promote brazing material retention in the joint area and impart additional strength to the joint [10].

Traditional surface roughening or texturing methods typically involve mechanical machining and the use of etchants, but these approaches are often less effective for ceramic-based materials [11]. Non-contact technologies, such as those based on plasma and lasers [12], represent promising alternatives. Plasma processes are by now well-established, and are particularly valuable for surface preparation. They are frequently employed in both research and manufacturing for various purposes, such as decontamination and cleaning [13,14], surface activation [15], as well as roughening and texturing [16]. Moreover, different industries have made significant contributions to advancing plasma surface technologies [17–19].

Atmospheric Pressure Plasmas (APPs), such as corona plasma devices [20] and atmospheric-pressure plasma jets (APPJs) [21], involve simplified operations at atmospheric pressure, thus making them suitable for integration in automated production lines. Although widely used in the plastics industry for surface preparation, there are limited examples of their use for ceramics and glasses [22–24]. APPJs, which were specifically designed for efficient and uniform material treatments, generate plasma inside a torch, which is then expelled through an opening by means of a gas flow. Despite there being a small treatment area, scanning the surface overcomes this limitation, in the same way as laser treatments. Importantly, APPJs form a stable plasma plume, thereby distinguishing them from corona discharges [25].

Furthermore, after optimizing the process parameters and the working gases, APPJs can be used for reactive etching. As far as homogeneous materials are concerned, this process requires masking to transfer a pattern. On the other hand, composites, being composed of more constituents, each with its own structure and composition, provide diverse responses to physical and/or chemical environmental factors, thereby enabling selective removal. The selective removal process can result in several textures, according to the composite architecture, and these can result in a brush-like texture when the matrix or the fibers are selectively eroded.

Selective removal, which is based on thermal treatments, has been reported for SiC/SiC [26,27] and C/C [28], but since the entire volume of these composites is affected, their global performances can be worsened. For this reason, it is crucial to confirm that the treatment on the surface and the plasma treatments are perfect candidates for this scope, as reported in a previous work on surface modification of SiC and SiC/SiC joints [29].

The sensitivity of the carbon phases to oxidation offers opportunities to provide beneficial surface texturing on C/C, as demonstrated in two studies reported in the literature. A selective thermal treatment was exploited in Ref. [28], while the use of an air-based APPJ to produce a brush-like texture on C/SiC was described in Ref. [30]. In the latter case, the C/SiC texturization was achieved by removing C fibers from the surface, which led to an interlocking effect with the brazing alloy.

This work, which expands the available knowledge on APPJ texturing, focuses on the brush-like texturing of C/C to improve the joint performance of similar and dissimilar joints (C/C-copper). First, a screening study was conducted to select the most promising operating parameters for C/C texturing. Then, the wettability of a specific pretreated C/C surface by the well-known TiCuNi braze was evaluated. Finally, C/C–TiCuNi–C/C and C/C–TiCuNi–Cu joints were produced and characterized, in terms of interfacial reactivity and mechanical performance.

2. Materials and methods

The experimental activity was carried out on a 3D C/C composite (NB31) manufactured by SNECMA (France). The 3-dimensional architecture was manufactured with a combination of pitch-derived fibers along the Z axis, PAN-derived fibers along the X axis, and PAN-derived needles along the Y axis. The matrix, made of pyrolytic carbon, was manufactured by combining Chemical Vapor Infiltration (CVI) and pitch impregnation. NB31 composite has a density of 1.9 g cm^{-3} and open porosity of ~8 % [31]. Further information on the C/C used in this study is available in Ref. [32].

C/C composites were cut, using a diamond saw, into 10 mm × 10 mm samples, with a thickness of 5 mm. The effect of plasma was studied on the square section, i.e. the XY plane, perpendicular to the Z-aligned pitch fiber.

The choice of the surface that had to be treated was made on the basis of the results of previous research [33], which had targeted the joining of C/C to copper for ITER, to compare the results of the present study with those of [30]. In this work, the joint was manufactured using the same surface, since the thermal conductivity was higher along the X direction.

After cutting, the YZ surface was polished, using SiC sandpaper of up to a P2400 grit size, which corresponds to an average particle size of 6.5 μm, to obtain a uniform roughness for each sample.

The plasma treatment was delivered using an Atmospheric Pressure Plasma Jet (APPJ) device (PlasmaTec-X, Tantec, Denmark). The technical specifications of this device are available on the Tantec website [34,35]. The process parameters were: time, airflow (l/h), and nozzle-surface gap. The plasma gas consisted of compressed air, which was supplied at a minimum flow of 1000 l/h to prevent the nozzle from overheating. In this work, the nozzle-surface gap and the air flow were kept constant at 5 mm and 1750 l/h, respectively. Such settings were based on a previous study on the APPJ surface texturing of C/SiC [30]. However, the airflow was slightly increased to 1750 l/h to prevent any issues of nozzle overheating during the treatment. The plasma treatment was conducted for six different times: 30 s, 1 min, 5 min, 10 min, 15 min and 20 min, and each sample was weighed by means of a high-precision analytical scale before and after the treatment to measure the weight loss resulting from the oxidation of carbon. Furthermore, the etching depth was measured using a contact profilometer (Taylor Hobson, The UK). Three samples were investigated for each treatment time, and the average etch depth was then calculated. The surface temperature was recorded during the plasma treatment using a thermal imaging camera (FLIR E6, USA). Additionally, a K-type thermocouple was placed in contact with the sample.

Furthermore, the morphology of the XY surface was characterized, before and after the APPJ treatment, by means of a scanning electron microscope (JEOL benchtop equipped with EDS, The USA). This preliminary SEM characterization was used, together with the weight loss and etching depth data, to screen and select the most viable set of conditions in order to assess the effect of the treatment on the joint strength. As a result of this screening step, a treatment length of 30 s was selected for the subsequent characterization of the joints.

A confocal microscope (Sensofar S-neox, Spain) provided data on the evolution of the surface texture, and the obtained results were compared with those obtained by means of SEM.

The braze selected for manufacturing the C/C joints was TiCuNi alloy (70 wt% Ti, 15 wt% Cu, 15 wt% Ni), in the form of 50 μm thick foils produced by Wesgo (Germany). This braze is well-known as a joining material for non-oxide ceramics [7,36], and it was previously investigated in Ref. [37] for the manufacturing of C/C joints.

The wetting of TiCuNi on the C/C surface at 1000 °C was evaluated for both the untreated and 30 s APPJ treated samples. TiCuNi alloy was prepared by arc melting the appropriate quantities of the pure metals (purity >99.9 %) to obtain small spheric samples of about 0.3 g each. The TiCuNi sample was then placed onto the composite surface, and this

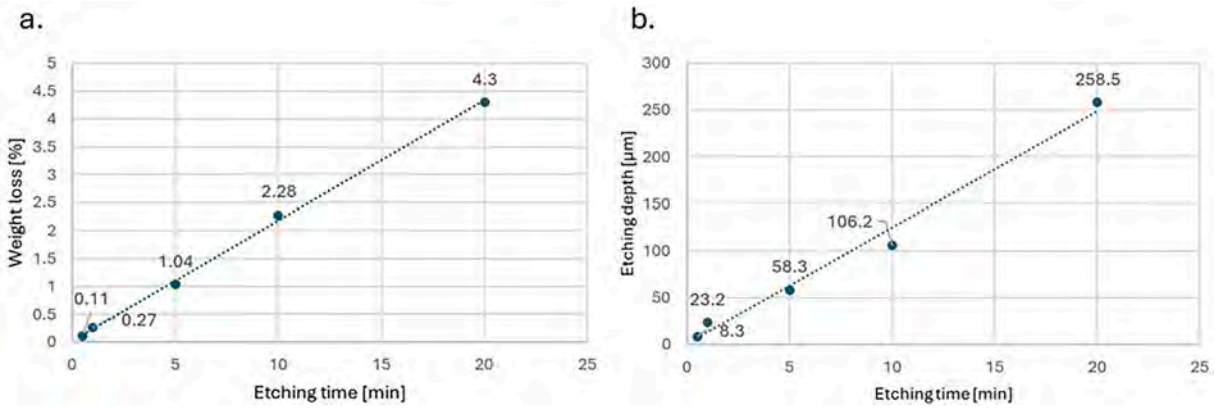

Fig. 1. Weight loss (a) and etching rate (b) curves under APPJ.

couple was then inserted into a vacuum furnace specifically designed for wetting tests at high temperatures. An internal camera collected frames of the evolution of the contact angle for about 20 min. After the tests, cross-sectioned samples were manufactured to observe the braze-C/C interface and evaluate the infiltration of the braze into the textured brush-like surface.

Both untreated and 30s APPJ treated similar (C/C–C/C) and dissimilar joints (C/C-copper) were obtained, by means of brazing, using three 50 µm thick foils of TiCuNi as an interlayer, without any external pressure. Three 50 µm foils were chosen to achieve a thickness of the seam of about 100 µm. The same strategy was used in Ref. [37]. The 10 mm × 10 mm samples were joined with an off-set of half their length

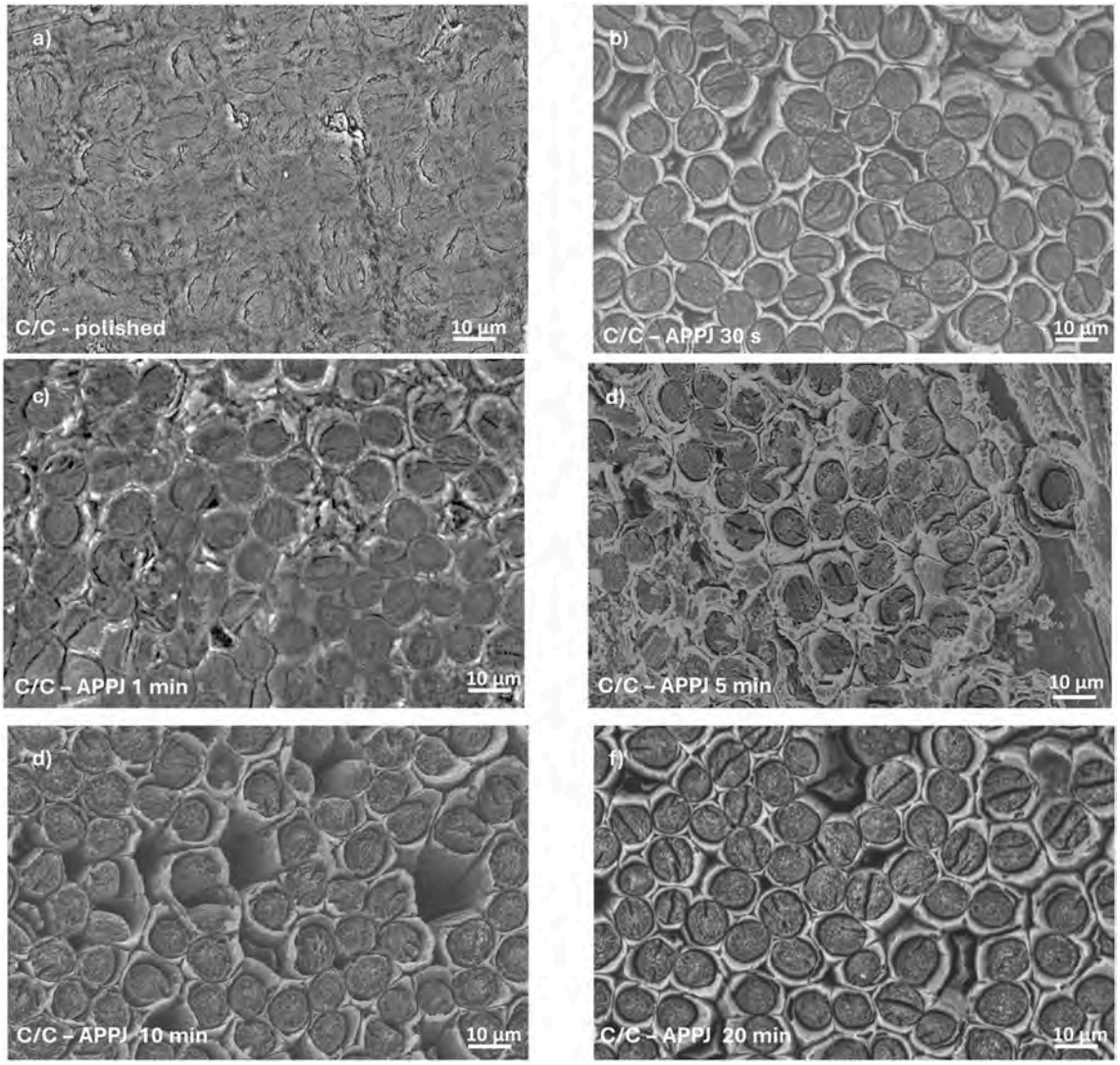

Fig. 2. SEM images of the top views of the C/C samples: polished (a), 30 s APPJ (b), 1 min APPJ (c), 5 min APPJ(d), 10 min APPJ (e), and 20 min APPJ (f).

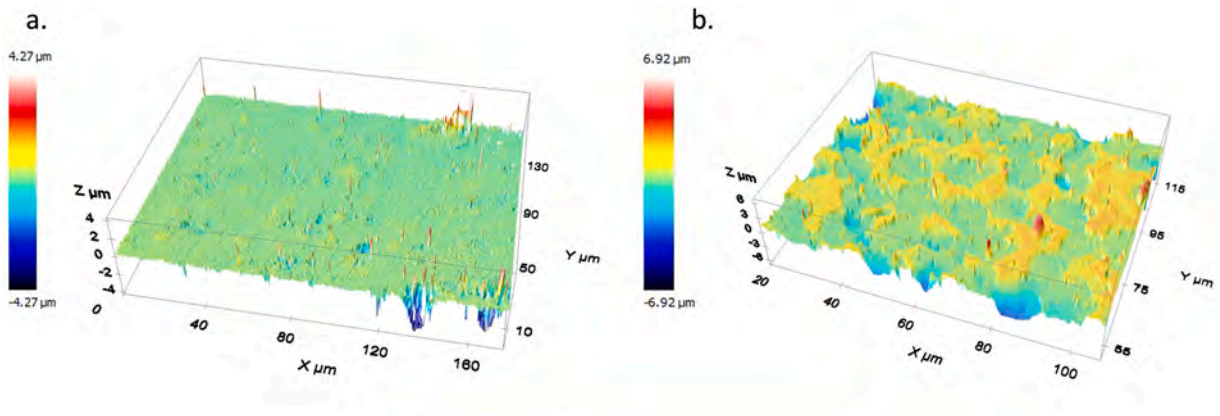

Sample	SdR
Polished C/C	11%
APPJ-treated C/C (30s)	190%

Fig. 3. Roughness maps of the polished C/C are illustrated in (a), while (b) shows those of the 30 s Atmospheric Pressure Plasma Jet (APPJ) treated C/C. The associated Sdr (surface roughness depth) values are reported beneath each map.

resulting in an approximately joining area of 50 mm^2. The samples were held at 1000 °C for 10 min, and a heating rate and cooling rate of 10 °C/min were applied. The joining process was carried out under vacuum (10^{-5} mbar) to prevent oxidation. The joined specimens were then mechanically tested, to measure the joint strength, using a single lap offset (SLO) test under compression. At least three samples were tested for each experimental condition to calculate the average shear strength. Further information on the SLO test configuration and geometries of the specimens can be found in Ref. [38]. The universal testing machine (SINTECH D/10) was equipped with a 50 kN load cell, and the crosshead speed was set at 1 mm/min. After failure, the fractured surfaces underwent a visual inspection, and SEM was used to observe their cross-sections in order to analyze the correlation between the joint microstructure and the mechanical properties.

3. Results and discussion

The XY surface of the pitch-fiber perpendicular C/C was treated using an APPJ treatment and different exposure times, as described in the experimental section. The mass loss and the evolution of the etching depth recorded for the different treatment-time lengths (30 s, 1 min, 5 min, 10 min, 20 min) are shown in Fig. 1. Both the mass loss and the etching depth increased linearly with the treatment time. The mass loss can be attributed to the oxidation of C, due to the interaction with plasma. The oxidation of carbon has been reported to start from 400 °C, at atmospheric pressure [39], but the temperature on the composite surface during the treatment was expected to be lower, according to the technical specification of the APPJ device. This was confirmed by observing the temperature measured by the thermal imaging camera and the K-type thermocouple, which measured a peak temperature of 250 °C close to the APPJ nozzle, while the temperature of the C/C samples never exceeded 200 °C. These values confirmed that the temperature was far lower than the threshold for thermal oxidation under atmospheric pressure.

The APPJ-enhanced oxidation can be justified by the presence of highly reactive oxygen-containing species (ROS), which can lower the threshold energy of the reaction. No compositional analysis was carried out on the plasma plume, but the formation of ROS in air-based atmospheric-pressure plasma has been extensively documented in the literature, where O_3, NO_x, atomic oxygen, OH radicals and other species have been identified as enablers of low-temperature oxidation [40,41]. APPJ-enhanced oxidation has been reported for polymeric materials, even for temperatures close to room temperature [42].

Fig. 2 reports top view SEM micrographs of the C/C surfaces before (Fig. 2a) and after the plasma treatments carried out for different durations of 30 s, 1 min, 5 min, 10 min, and 20 min (Fig. 2b-f).

As can be seen from the SEM micrographs (Fig. 2), the fibers appear to be preferentially etched, thus pointing to a moderately higher oxidizing effect on the fibers.

Annular gaps formed around the C fibers, as has frequently been reported after thermal oxidation but, in this case, no visible sharpening effect was observed [43]. On the contrary, after plasma etching, the fibers showed a nearly flat surface, characterized by the presence of uniformly distributed porous channels, as can be seen for all the treated samples in Fig. 2.

The surface of polished C/C shows the fibers and the matrix at the same height. After 30 s of APPJ treatment, the fibers are found on a lower plane than the matrix, resulting in a brush-like texture. With extended plasma treatment, although material removal continues (Fig. 1), no further changes in the brush-like structure were observed, suggesting that the etching rate of the matrix and fibers remains constant. The brush-like structure likely forms before 30 s and remains nearly unchanged even as the treatment time increases.

The condition of the sample at 30 s was determined to be the most closely aligned with the aim of identifying a treatment protocol that would be both effective and time-efficient, while at the same time minimizing detrimental effects on the composite properties. Consequently, this condition was chosen as the pre-bonding treatment for the subsequent characterization and brazing tests.

The surface topography was characterized by three distinct contributions that described its deviation from an ideal plane: the predominant pattern, roughness (distribution of irregularities), and waviness. Greater deviations from the ideal planar surface would result in a larger contact area being available for the adhesive. Consequently, increasing the roughness before joining could lead to an improved performance of the joined component. A random increase in roughness generally has a positive effect on interlocking, as a well-distributed texture is formed on the surface, which, in turn, is expected to have a further positive effect, i.e., an increased joining material retention and homogeneous infiltration of the brazing alloy.

The surface topography of the 30 s APPJ treated C/C was characterized by means of confocal microscope profilometry. The results confirmed the presence of a preferential etching of the fibers. Roughness maps of the C/C surfaces, before and after the plasma treatment, are

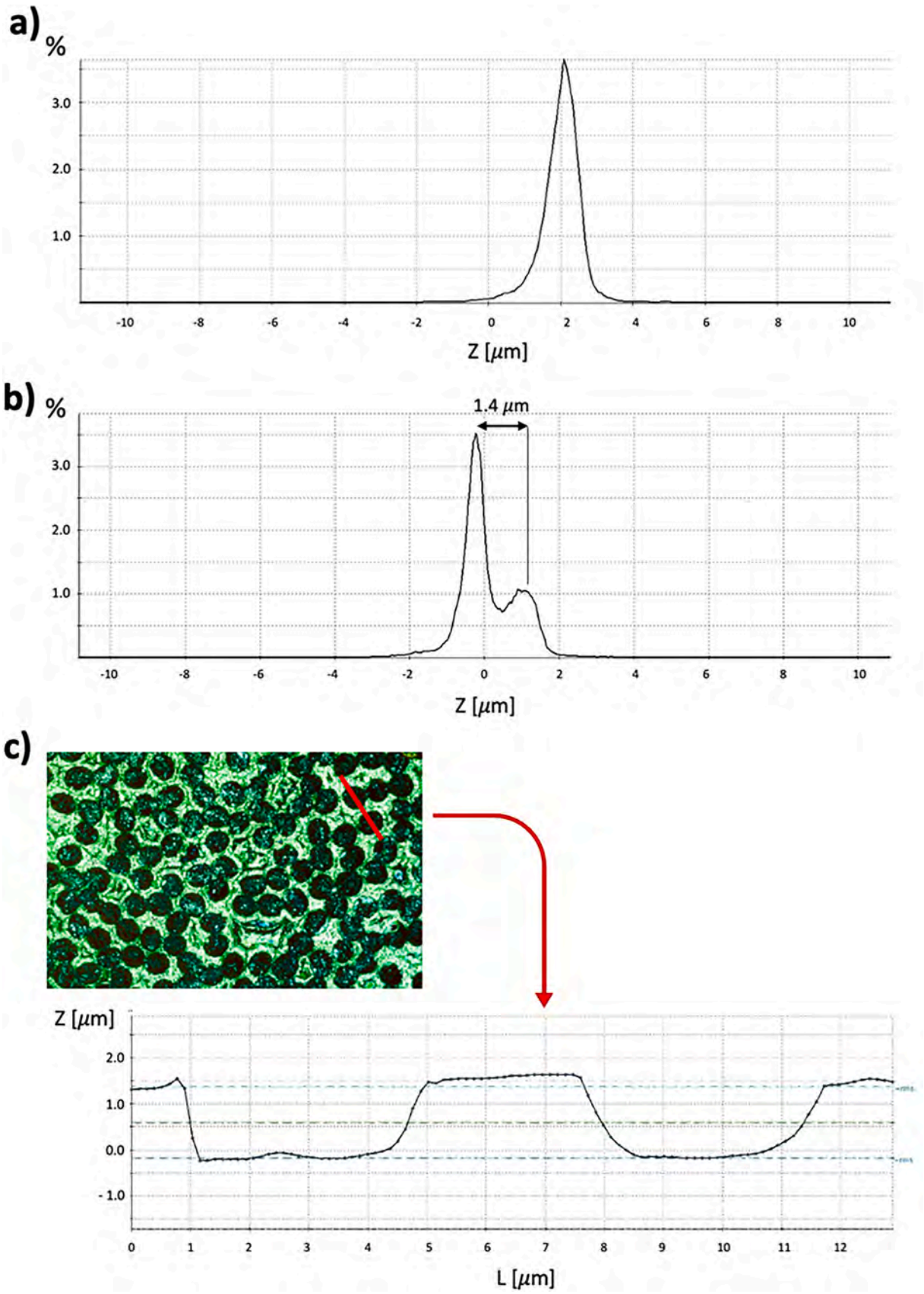

Fig. 4. The height distribution (expressed as % of points acquired at a given height) of polished C/C is presented in (a), while (b) illustrates the height distribution of C/C after a 30 s APPJ treatment. Additionally, (c) shows the results of confocal line analysis on the C/C surface treated with APPJ for 30 s. The reported profile corresponds to the line identified by the segment.

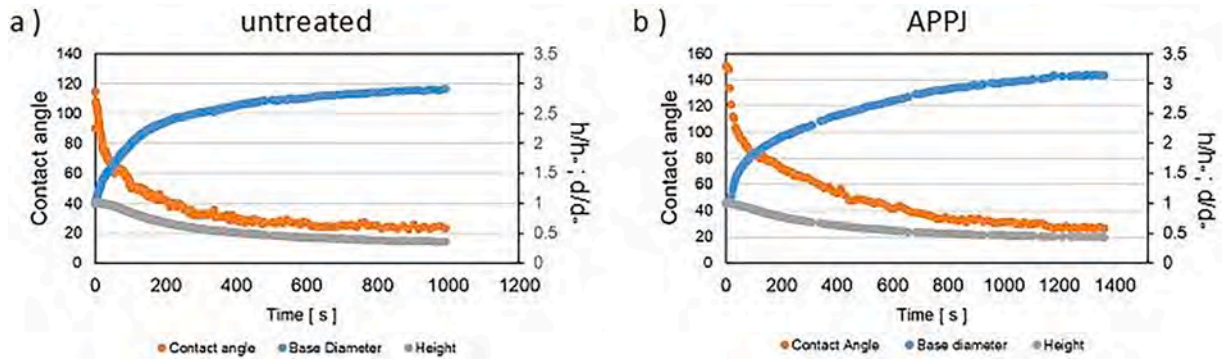

Fig. 5. The evolution of the contact angle (left axis) and the normalized drop dimensions, base diameter, and height (right axis) of the liquid TiCuNi tested on the untreated C/C (a) and on the C/C after a 30-s Atmospheric Pressure Plasma Jet (APPJ) treatment (b).

presented in Fig. 3. These maps confirm the deductions made on the scanning electron microscope inspections. The alteration of the surface texture induced by APPJ exposure is discernible, with fibers that exhibit a reduced height, compared to the matrix points, a result of significant importance. The erosion of fibers appears to be uniformly distributed on the surface, and this has led to the formation of dispersed cavities.

The developed interfacial area ratio (Sdr) parameter, reported as in eq (1), was used to evaluate the evolution of the texture after the APPJ treatment.

$$Sdr = \frac{Real\ surface - Ideal\ surface}{Ideal\ surface} \quad (1)$$

Sdr offers preliminary information on the changes of roughness and of the specific area. The minimum value (0) is associated with a perfectly flat surface, while increasing values describe deviations from the ideal plane. Therefore, such a parameter is critical for evaluating the roughness of the C/C surface before and after APPJ, and to determine the texturing effects of the plasma treatment. The pristine surface exhibited an Sdr value of 11 %. Following a 30 s exposure to APPJ, the Sdr value increased significantly to 190 %, thereby indicating a remarkable increase in the surface area. Furthermore, the analysis of the height distribution showed a marked disparity in the distribution observed between the untreated and the APPJ treated C/Cs. The untreated samples exhibited a single-peak distribution, as can be seen in Fig. 4a. The treated C/C instead showed a double-peak curve (Fig. 4b). The highest peak corresponded to the fibers (lowest points), and the other corresponded to the matrix. This dual-peak pattern indicates a clear demarcation between the two constituents and offers a precise delineation of the morphological changes induced by the APPJ treatment. The calculated average height gap between the fibers and the matrix, after the plasma-enhanced selective removal, was 1.4 μm. Similar observations were made in the line analysis illustrated in Fig. 4c,

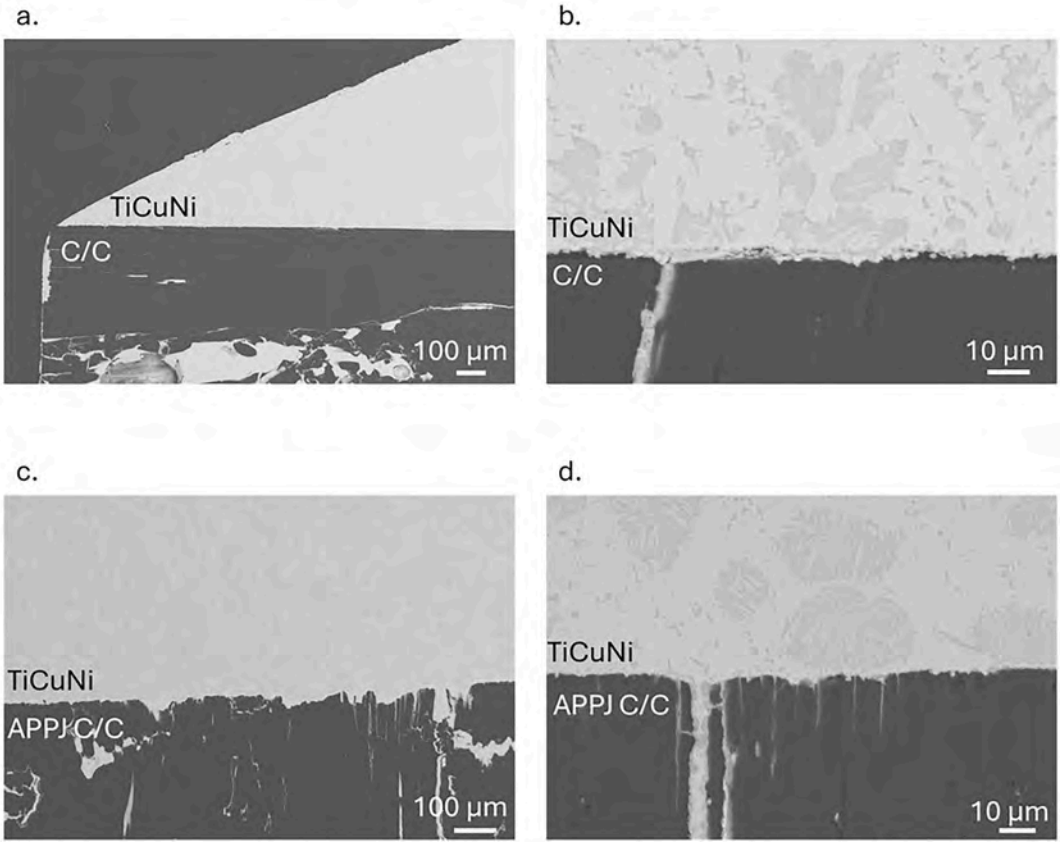

Fig. 6. Cross-sections of the untreated C/C (a,b) and the 30 s APPJ-treated C/C (c,d) after the TiCuNi wetting tests.

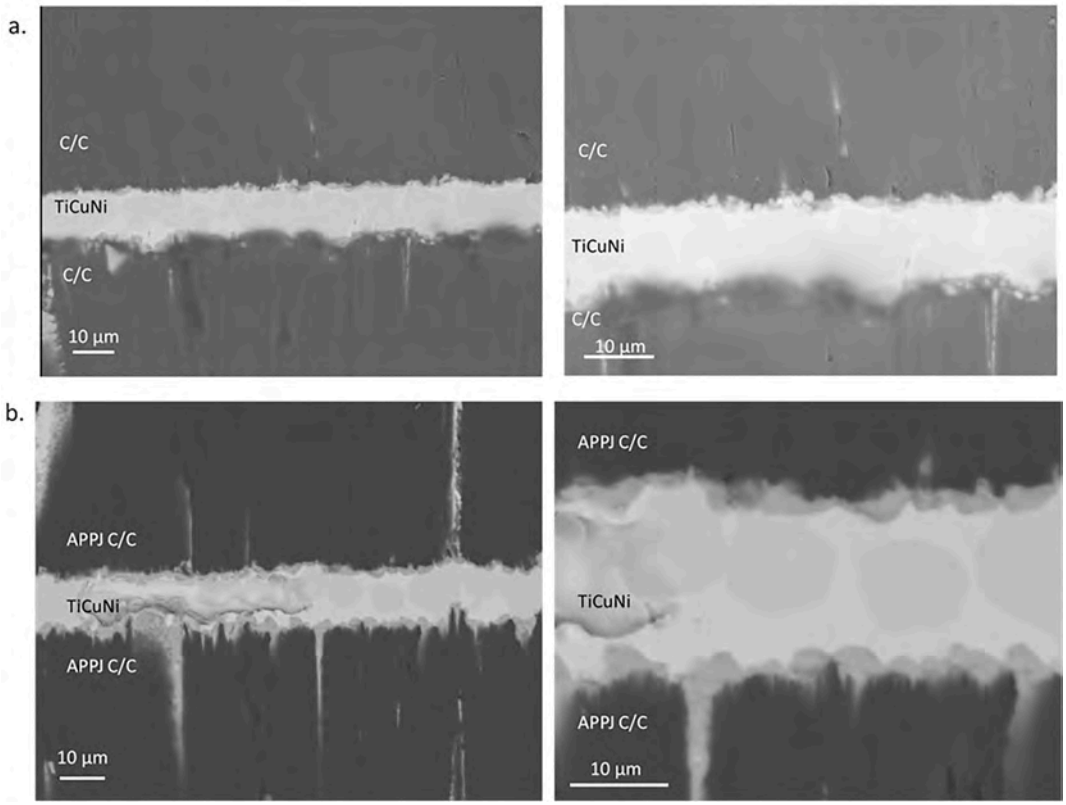

Fig. 7. Cross-sections of the joined untreated C/C (a,b) and the joined 30 s APPJ C/C (c,d).

which was conducted to measure the surface profile. Steps between the matrix and fibers are discernible, and the profile appears brush-like, in accordance with the targeted modification.

The SEM analysis and profilometer characterizations unequivocally validated the efficacy of the APPJ treatment in creating the intended brush-like structure on the composite surface.

The subsequent step of the experimental investigation was concentrated on assessing how this new surface texture influenced the interaction with the liquid TiCuNi brazing alloy and on the strength of the brazed composites. Fig. 5 illustrates the evolution of the contact angles and drop dimensions vs. time for the polished C/C and for the 30 s APPJ treated C/C. No discernible differences were observed for the two types of substrate: the wetting kinetics was observed to reach equilibrium contact angles of 23° and 25° for the polished C/C and APPJ C/C, respectively. The wetting and spreading sequence of the liquid TiCuNi alloy on the modified C/C composites was as follows: the liquid brazing alloy completely filled the gaps between the fibers and the matrix and then moved forward during the spreading process. It can be speculated that there was no priority of spreading in the case of the treated surfaces. In fact, such behavior did not lead to an enhanced contact angle of the brazing alloy on the treated C/C surfaces, compared to the contact angle of TiCuNi on the surface of the non-modified C/C.

Following the wettability tests, the samples underwent cross-cutting to examine the interface between TiCuNi and the composite (Fig. 6). The solidified drop was formed by two phases, namely Ti2(Ni,Cu) (light phase in microstructures of Fig. 6a–d), and Ti with Cu and Ni dissolved (dark phase) consistently with the eutectic in the ternary Cu–Ni–Ti system [44]. No evident TiC layer was detected consistently with the low kinetics of formation of this compound [44]; no other phases are foreseen by the phase diagrams. Certain large voids and porosities were present in the composite before the plasma treatment, as a result of the manufacturing process, and these were entirely filled by the braze material, as can be seen in Fig. 6a and, at higher magnification, in Fig. 6b. It should be noted that new infiltration channels were observed in the plasma treated samples, thereby indicating that the newly induced texture could enhance alloy infiltration and, consequently, promote an interlocking mechanism (Fig. 6 c-d). The wetting results and the consequent microstructural analysis are consistent with previous studies concerning the wetting of liquid TiCuNi on pure porous graphite at 1000 °C [44].

Moreover, in Ref. [26], the authors reported a decrease in the wettability of the brazing on a modified (in this case oxidized) C/C composite surface and a subsequent contact angle increase.

On the other hand, the C/C surface modified using APPJ exhibited a favorable wettability. The surface modification, which facilitated the penetration of the liquid brazing alloy into the gaps, did not impede the spreading and wetting of TiCuNi.

Cross-sections of C/C–C/C joined samples for both the untreated and APPJ treated surfaces are reported in Fig. 7: the microstructures and compositions are similar to those reported for the wetting tests. The joint thickness was found to be approximately 10 µm for both the treated and untreated samples; this thickness is significantly thinner than that of the starting interlayer, which consisted of a stack of three 50 µm-thick TiCuNi foils. This indicates a comparable degree of infiltration of the composite into the voids and a similar depletion of the joining material from the joint area.

The joint interface of the untreated C/C exhibited a relatively flat profile, while the APPJ treated C/C displayed a distinctive brush-like structure and an enhanced interlocking with the braze. In both cases, a very thin reactive TiC layer formed at the interface with the composite (EDS analysis not reported here).

In addition, the infiltration of the liquid TiCuNi alloy into the annular gaps during the brazing process preferentially occurred at the area where carbon fibers were perpendicular to the composite surface.

Salvo et al. [37], in their study on C/C samples joined with three TiCuNi foils, reported a joint thickness that ranged from 90 to 100 µm and a joint strength of 17 ± 3 MPa after an SLO shear stress test. A higher joint strength of 24 ± 2 MPa was achieved for a single TiCuNi foil, which

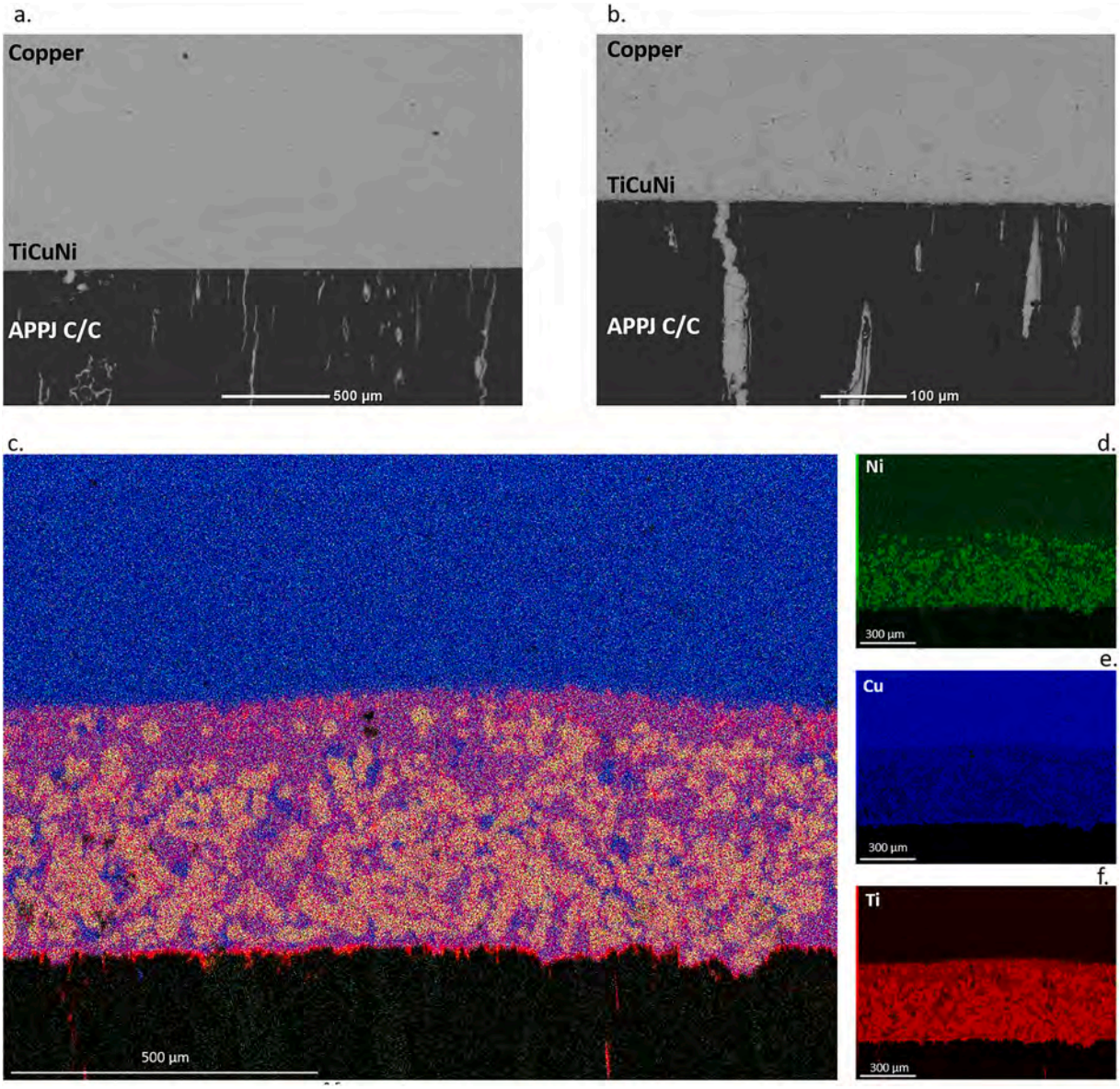

Fig. 8. Cross-section of the TiCuNi joined APPJ C/C-copper under different magnifications (a) and (b). Elemental mapping of the cross-section of a C/C–TiCuNi–Cu joined sample (red: Ti; blue: Cu; green: Ni) (c–f). (For interpretation of the references to colour in this figure legend, the reader is referred to the Web version of this article.)

resulted in a final thickness of 30–35 µm. However, those results refer to C/C composites that were less porous than the ones considered here, and therefore resulted in a much lower infiltration of the braze into the composites.

The mechanical performance assessments, by means of SLO tests, indicated significantly lower values than those reported in Ref. [31] for both the untreated and treated samples. The apparent shear strength of the untreated samples was 2.3 ± 0.8 MPa, while the treated samples exhibited a similar value of 2.0 ± 0.3 MPa. In both cases, cohesive failure was evident, with the joining material present on each fracture surface. Moreover, the textured samples displayed a larger amount of braze on the surface, likely due to its enhanced retention.

Although cohesive failure usually suggests an optimal adhesion with the substrate, which implies a high mechanical performance, the observed low performance and similar behavior between the treated and untreated samples may be attributed to an insufficient quantity of brazing alloy in the joint. The use of three TiCuNi foils may have been inadequate to effectively join these composites along the ZY face. Although increasing the number of foils could provide a larger reservoir of the joining material, it might not be a practical solution.

Although surface texturing was successfully achieved on C/C, thereby suggesting an excellent treatment efficacy, the C/C–C/C joints did not show any significant improvements, due to the excessive infiltration problems in the composite. As mentioned in the introductory section, numerous studies have been conducted on C/C dissimilar joints, i.e. C/C to metal junctions. For this reason, the effect of such a treatment was also evaluated for C/C to copper joints in order to gather data on the evolution of the joint strength obtained from the APPJ treatment for a different coupling. To this aim, SLO mechanical tests were performed on TiCuNi joined C/C-copper.

In the case of C/C–C/C, the joint was depleted of the braze because of the presence of cavities on both parts and capillarity effects promoted by the vacuum degree applied during the process. As far as the C/C–Cu joints are concerned, as no infiltration of braze occurred in the copper plate, the depletion was confined to the C/C side. Furthermore, the starting ternary eutectic TiCuNi [45] was further enriched in Cu by means of dissolution: for this reason, the resulting interface between the copper and TiCuNi could not be distinguished after the joining process,

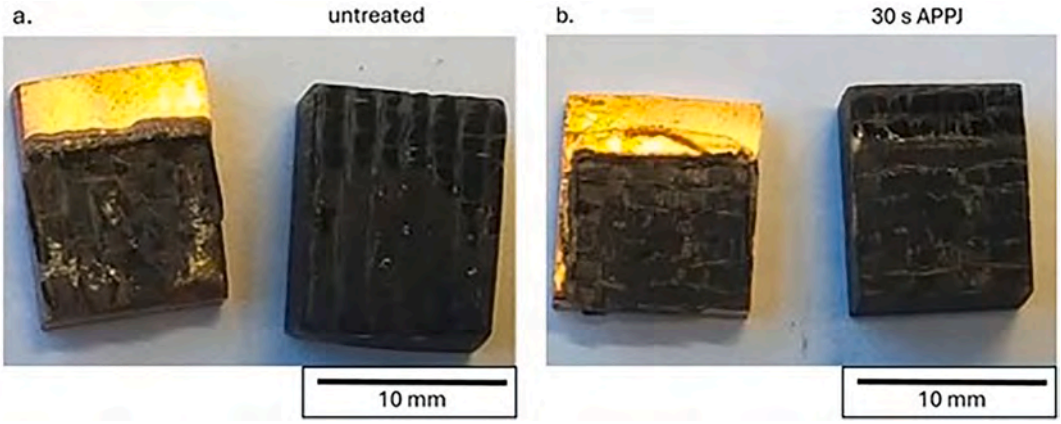

Fig. 9. Failure surfaces of the untreated C/C-copper (a) and treated C/C-copper (b).

as can be seen in the SEM micrographs shown in Fig. 8. To estimate the thickness of the final interlayer in dissimilar joints, we carried out an element mapping of a cross-section (Fig. 8c). The brazing alloy was applied using three 50-μm foils, while the area containing Ti, Cu, and Ni extends over 400 μm, resulting in the formation of a Ti- and Ni-rich layer. Consequently, an extensive interlayer is created by the diffusion of the brazing alloy elements into the copper adherend.

Mechanical tests revealed an increase in joint strength for the plasma treated C/C. The untreated C/C–Cu joined samples failed at $\tau = 9.5 \pm 5.6$ MPa, whereas the APPJ-treated C/C-copper samples showed a significantly higher strength, $\tau = 22.8 \pm 6.9$ MPa, thus indicating a 140 % improvement over the untreated composite. The relatively high standard deviations of the different samples could be attributed to variations in the distribution of the fibers on the surfaces.

Delamination of C/C was observed in both sets of samples (Fig. 9). The enhanced mechanical strength of the APPJ-treated C/C-copper may be attributed to a more pronounced interlocking effect, as a result of the improved infiltration of the braze into the brush-like texture.

The promising results obtained for C/C–Cu suggest that if the issue of joining material depletion in C/C–C/C joints with a brush-like texture were to be addressed, higher mechanical performances could be achieved.

4. Conclusions

The activities presented in this paper offer the first insights into the use of APPJ as an effective and versatile pre-joining treatment for the manufacturing of C/C parts, thereby opening new research opportunities on CMCs and delivering helpful information to industry.

In fact, the use of Atmospheric Pressure Plasma Jet (APPJ) has been proven to be effective in the surface texturing of C/C. Different etching rates were observed for the matrix and the fibers when exposed to the plasma. Remarkably, a brush-like texture on the C/C surface was achieved with a plasma treatment of only 30 s. Although the texture did not impact the evolution of the contact angle of the studied brazing alloy to any great extent, it introduced additional anchoring points on the surface, thereby leading to a substantial increase in the surface area. These findings suggest the potential for an improved joint strength of brazed C/C–C/C samples. However, mechanical tests revealed poor performances of both treated and untreated samples. These low joint strengths have been attributed to the extensive infiltration of TiCuNi into the existing cavities of C/C, which resulted in the depletion of the braze in the joining area and in a final joint thickness of about 10 μm. Further optimization of the brazing process and consideration of a different brazing alloy may be necessary to improve the mechanical performance of similar C/C joints. On the other hand, a 140 % improvement over the untreated composite was observed for dissimilar C/C–Cu joints manufactured with plasma-treated composites, due to the interlocking effect induced by C/C texturing. In this latter case, the dissolution of Cu in the liquid TiCuNi led to a limited infiltration in the counterpart C/C.

In short, the improvement in joint strength caused by the APPJ treatment of the C/C composites, at least in the case of dissimilar joints (C/C–Cu), could be attributed to the increased bonding area as a result of the formation of annular gaps around the C fibers, to an increased retention of the brazing material at the joint interface, and to the enhanced pinning effect induced by the infiltrated brazing alloy.

The here presented research on the APPJ surface texturing of C/C was primarily based on experimental observations. Further activities, in which the experimental findings could be combined with theoretical modeling, may enhance the knowledge on this topic and contribute to the development of more effective and controlled surface texturing processes.

CRediT authorship contribution statement

Alessandro De Zanet: Writing – review & editing, Writing – original draft, Methodology, Investigation, Formal analysis, Data curation, Conceptualization. **Fabrizio Valenza:** Writing – review & editing, Writing – original draft, Validation, Supervision, Methodology, Investigation, Formal analysis, Data curation, Conceptualization. **Valentina Casalegno:** Writing – review & editing, Supervision, Resources, Project administration, Funding acquisition, Conceptualization. **Sofia Gambaro:** Writing – review & editing, Writing – original draft, Validation, Methodology, Investigation, Formal analysis, Conceptualization. **Fabiana D'Isanto:** Investigation, Formal analysis, Data curation. **Milena Salvo:** Writing – review & editing, Validation, Supervision, Resources, Conceptualization.

Declaration of competing interest

The authors declare the following financial interests/personal relationships which may be considered as potential competing interests: Valentina Casalegno reports financial support was provided by European Union - NextGenerationEU (Grant agreement no. ECS00000036). If there are other authors, they declare that they have no known competing financial interests or personal relationships that could have appeared to influence the work reported in this paper.

Acknowledgment

This publication is part of the NODES project which has received funding from the MUR – M4C2 1.5 of PNRR funded by the European Union - NextGenerationEU (Grant agreement no. ECS00000036).

References

[1] C. Scarponi, Carbon–carbon composites in aerospace engineering, in: Adv. Compos. Mater. Aerosp. Eng., Elsevier, 2016, pp. 385–412, https://doi.org/10.1016/B978-0-08-100037-3.00013-4.

[2] T. Hirai, S. Panayotis, V. Barabash, C. Amzallag, F. Escourbiac, A. Durocher, M. Merola, J. Linke, T. Loewenhoff, G. Pintsuk, M. Wirtz, I. Uytdenhouwen, Use of tungsten material for the ITER divertor, Nucl. Mater. Energy. 9 (2016) 616–622, https://doi.org/10.1016/j.nme.2016.07.003.

[3] J. Linke, J. Du, T. Loewenhoff, G. Pintsuk, B. Spilker, I. Steudel, M. Wirtz, Challenges for plasma-facing components in nuclear fusion, Matter Radiat. Extremes 4 (2019) 056201, https://doi.org/10.1063/1.5090100.

[4] M. Salvo, V. Casalegno, S. Rizzo, F. Smeacetto, M. Ferraris, M. Merola, One-step brazing process to join CFC composites to copper and copper alloy, J. Nucl. Mater. 374 (2008) 69–74, https://doi.org/10.1016/j.jnucmat.2007.07.010.

[5] P. Appendino, M. Ferraris, V. Casalegno, M. Salvo, M. Merola, M. Grattarola, Direct joining of CFC to copper, J. Nucl. Mater. 329–333 (2004) 1563–1566, https://doi.org/10.1016/j.jnucmat.2004.04.313.

[6] S. Roccella, E. Cacciotti, D. Candura, A. Mancini, A. Pizzuto, A. Reale, A. Tatì, E. Visca, Ultrasonic test of carbon composite/copper joints in the ITER divertor, Fusion Eng. Des. 88 (2013) 1802–1807, https://doi.org/10.1016/j.fusengdes.2013.05.078.

[7] X. Song, H. Li, V. Casalegno, M. Salvo, M. Ferraris, X. Zeng, Microstructure and mechanical properties of C/C composite/Ti6Al4V joints with a Cu/TiCuZrNi composite brazing alloy, Ceram. Int. 42 (2016) 6347–6354, https://doi.org/10.1016/j.ceramint.2016.01.026.

[8] A.A. Shokati, N.Y. Zhou, J.Z. Wen, Dissimilar joining of carbon/carbon composites to Ti6Al4V using reactive resistance spot welding, J. Alloys Compd. 772 (2019) 418–428, https://doi.org/10.1016/j.jallcom.2018.09.018.

[9] Z. Yi, L. Ran, M. Yi, Differences in microstructure and properties of C/C composites brazed with Ag-Cu-Ti and Ni-Cr-P-Ti pasty brazing filler, Vacuum 168 (2019) 108804, https://doi.org/10.1016/j.vacuum.2019.108804.

[10] S.J. Marshall, S.C. Bayne, R. Baier, A.P. Tomsia, G.W. Marshall, A review of adhesion science, Dent. Mater. 26 (2010) e11–e16, https://doi.org/10.1016/j.dental.2009.11.157.

[11] S.N. Grigoriev, T.N. Soe, K. Hamdy, Y. Pristinskiy, A. Malakhinsky, I. Makhadilov, V. Romanov, E. Kuznetsova, P. Podrabinnik, A.Y. Kurmysheva, A. Smirnov, N. W. Solís Pinargote, The influence of surface texturing of ceramic and superhard cutting tools on the machining process—a review, Materials 15 (2022) 6945, https://doi.org/10.3390/ma15196945.

[12] A. De Zanet, V. Casalegno, M. Salvo, Laser surface texturing of ceramics and ceramic composite materials – a review, Ceram. Int. 47 (2021) 7307–7320, https://doi.org/10.1016/j.ceramint.2020.11.146.

[13] F. Rossi, O. Kylián, M. Hasiwa, Decontamination of surfaces by low pressure plasma discharges, Plasma Process. Polym. 3 (2006) 431–442, https://doi.org/10.1002/ppap.200600011.

[14] A. Belkind, S. Krommenhoek, H. Li, Z. Orban, F. Jansen, Removal of oil from metals by plasma techniques, Surf. Coating. Technol. 68–69 (1994) 804–808, https://doi.org/10.1016/0257-8972(94)90257-7.

[15] R. Ghobeira, P.S. Esbah Tabaei, R. Morent, N. De Geyter, Chemical characterization of plasma-activated polymeric surfaces via XPS analyses: a review, Surface. Interfac. 31 (2022) 102087, https://doi.org/10.1016/j.surfin.2022.102087.

[16] G. Franz, Plasma roughening of polished SiC substrates, Mater. Sci. Semicond. Process. 5 (2002) 525–527, https://doi.org/10.1016/S1369-8001(02)00115-4.

[17] J. Izdebska-Podsiadły, Application of plasma in printed surfaces and print quality, in: Non-Thermal Plasma Technol. Polym. Mater., Elsevier, 2019, pp. 159–191, https://doi.org/10.1016/B978-0-12-813152-7.00006-8.

[18] A.S. Katsigiannis, N. Hojnik, M. Modic, D.L. Bayliss, J. Kovač, J.L. Walsh, Continuous in-line decontamination of food-processing surfaces using cold atmospheric pressure air plasma, Innovat. Food Sci. Emerg. Technol. 81 (2022) 103150, https://doi.org/10.1016/j.ifset.2022.103150.

[19] C. Gleissner, J. Landsiedel, T. Bechtold, T. Pham, Surface activation of high performance polymer fibers: a review, Polym. Rev. 62 (2022) 757–788, https://doi.org/10.1080/15583724.2022.2025601.

[20] J. Izdebska, Corona treatment, in: Print. Polym., Elsevier, 2016, pp. 123–142, https://doi.org/10.1016/B978-0-323-37468-2.00008-7.

[21] A. Schutze, J.Y. Jeong, S.E. Babayan, Jaeyoung Park, G.S. Selwyn, R.F. Hicks, The atmospheric-pressure plasma jet: a review and comparison to other plasma sources, IEEE Trans. Plasma Sci. 26 (1998) 1685–1694, https://doi.org/10.1109/27.747887.

[22] Y. Komagata, H. Ikeda, Y. Fujio, Y. Nagamatsu, H. Shimizu, Surface modification of feldspar porcelain by corona discharge and its effect on bonding to resin cement with silane coupling agent, J. Mech. Behav. Biomed. Mater. 105 (2020) 103708, https://doi.org/10.1016/j.jmbbm.2020.103708.

[23] A. De Zanet, M. Salvo, V. Casalegno, Surface modification of SiC to improve joint strength via a Corona plasma treatment, Ceram. Int. 48 (2022) 23492–23497, https://doi.org/10.1016/j.ceramint.2022.04.344.

[24] H. Ikeda, D. Sakai, S. Funatsu, K. Yamamoto, T. Suzuki, K. Harada, J. Nishii, Generation of alkali-free and high-proton concentration layer in a soda lime glass using non-contact corona discharge, J. Appl. Phys. 114 (2013) 063303, https://doi.org/10.1063/1.4817760.

[25] U. Lommatzsch, D. Pasedag, A. Baalmann, G. Ellinghorst, H.-E. Wagner, Atmospheric pressure plasma jet treatment of polyethylene surfaces for adhesion improvement, Plasma Process. Polym. 4 (2007) S1041–S1045, https://doi.org/10.1002/ppap.200732402.

[26] F. Valenza, V. Casalegno, S. Gambaro, M.L. Muolo, A. Passerone, M. Salvo, M. Ferraris, Surface engineering of SiCf/SiC composites by selective thermal removal, Int. J. Appl. Ceram. Technol. 14 (2017) 287–294, https://doi.org/10.1111/ijac.12618.

[27] V. Casalegno, F. Valenza, C. Balagna, R. Sedlák, V. Girman, M. Salvo, S. De la Pierre des Ambrois, M. Ferraris, Characterisation of joined surface modified SiCf/SiC composites, Ceram. Int. 46 (2020) 4159–4166, https://doi.org/10.1016/j.ceramint.2019.10.133.

[28] Z.W. Yang, C.L. Wang, Y. Han, Y.T. Zhao, Y. Wang, D.P. Wang, Design of reinforced interfacial structure in brazed joints of C/C composites and Nb by pre-oxidation surface treatment combined with in situ growth of CNTs, Carbon N. Y. 143 (2019) 494–506, https://doi.org/10.1016/j.carbon.2018.11.047.

[29] A. De Zanet, M. Pedroni, M. Salvo, E. Vassallo, V. Casalegno, Plasma etching as a surface engineering technique for SiC/SiC composites to improve joint strength, Ceram. Int. (2022), https://doi.org/10.1016/j.ceramint.2022.11.248.

[30] A. De Zanet, F. Valenza, V. Casalegno, S. Gambaro, M. Salvo, Atmospheric pressure plasma jet for surface texturing of C/SiC, Ceram. Int. 49 (2023) 32136–32143, https://doi.org/10.1016/j.ceramint.2023.07.182.

[31] K. Sugiyama, V.K. Alimov, J. Roth, Long-term deuterium release from CFC NB31 in the air atmosphere, Phys. Scripta T138 (2009) 014026, https://doi.org/10.1088/0031-8949/2009/T138/014026.

[32] T. Marshall, R. Pawelko, R. Anderl, G. Smolik, B. Merrill, R. Moore, D. Petti, Oxygen reactivity of a carbon fiber composite, Fusion Eng. Des. 69 (2003) 663–667, https://doi.org/10.1016/S0920-3796(03)00204-7.

[33] P. Appendino, M. Ferraris, V. Casalegno, M. Salvo, M. Merola, M. Grattarola, Proposal for a new technique to join CFC composites to copper, J. Nucl. Mater. 348 (2006) 102–107, https://doi.org/10.1016/j.jnucmat.2005.09.007.

[34] Tantec, PlasmaTec-X - Atmospheric Plasma: Product Information, (n.d.). https://www.tantec.com/wp-content/uploads/2020/05/PlasmaTEC-X-GB.pdf.

[35] Tantec SpotTEC - product information, (n.d.). https://mk0tantec25go4oy6kbt.kinstacdn.com/wp-content/uploads/2020/06/SpotTEC-GB.pdf (accessed 9 October 2021).

[36] M. Singh, R. Asthana, T.P. Shpargel, Brazing of carbon–carbon composites to Cu-clad molybdenum for thermal management applications, Mater. Sci. Eng. 452–453 (2007) 699–704, https://doi.org/10.1016/j.msea.2006.11.031.

[37] M. Salvo, V. Casalegno, Y. Vitupier, L. Cornillon, L. Pambaguian, M. Ferraris, Study of joining of carbon/carbon composites for ultra stable structures, J. Eur. Ceram. Soc. 30 (2010) 1751–1759, https://doi.org/10.1016/j.jeurceramsoc.2009.12.013.

[38] M. Salvo, V. Casalegno, S. Rizzo, F. Smeacetto, A. Ventrella, M. Ferraris, Glasses and Glass-Ceramics as Brazing Materials for High-Temperature Applications, Woodhead Publishing Limited, 2013, https://doi.org/10.1533/9780857096500.3.525.

[39] L. Xiaowei, R. Jean-Charles, Y. Suyuan, Effect of temperature on graphite oxidation behavior, Nucl. Eng. Des. 227 (2004) 273–280, https://doi.org/10.1016/j.nucengdes.2003.11.004.

[40] J.-H. Lee, K.-N. Kim, Effects of a nonthermal atmospheric pressure plasma jet on human gingival fibroblasts for biomedical application, BioMed Res. Int. 2016 (2016) 1–9, https://doi.org/10.1155/2016/2876916.

[41] G.E. Conway, A. Casey, V. Milosavljevic, Y. Liu, O. Howe, P.J. Cullen, J.F. Curtin, Non-thermal atmospheric plasma induces ROS-independent cell death in U373MG glioma cells and augments the cytotoxicity of temozolomide, Br. J. Cancer 114 (2016) 435–443, https://doi.org/10.1038/bjc.2016.12.

[42] K.G. Kostov, T.M.C. Nishime, A.H.R. Castro, A. Toth, L.R.O. Hein, Surface modification of polymeric materials by cold atmospheric plasma jet, Appl. Surf. Sci. 314 (2014) 367–375, https://doi.org/10.1016/j.apsusc.2014.07.009.

[43] G.L. Vignoles, J. Lachaud, Y. Aspa, J.-M. Goyhénèche, Ablation of carbon-based materials: multiscale roughness modelling, Compos. Sci. Technol. 69 (2009) 1470–1477, https://doi.org/10.1016/j.compscitech.2008.09.019.

[44] F. Valenza, S. Gambaro, A. Bigos, P. Czaja, M. Janusz-Skuza, J. Wojewoda-Budka, Wetting and interfacial reactivity of graphite by liquid TiCuNi, Surface. Interfac. 41 (2023) 103323, https://doi.org/10.1016/j.surfin.2023.103323.

[45] V.N. Eremenko, Y.I. Buyanov, S.B. Prima, Phase diagram of the system titanium-copper, Sov, Powder Metall. Met. Ceram. 5 (1966) 494–502, https://doi.org/10.1007/BF00775543.